www.ietdl.org

Published in IET Wireless Sensor Systems
Received on 29th October 2012
Revised on 12th February 2013
Accepted on 19th March 2013
doi: 10.1049/iet-wss.2012.0136

ISSN 2043-6386

Wireless walker dynamometer design and static calibration based on ant colony system

Rui Xu, Dong Ming, Shuang Qiu, Xin Wang, Hongzhi Qi, Lixin Zhang, Baikun Wan

Department of Biomedical Engineering, College of Precision Instruments and Optoelectronics Engineering, Tianjin University, Tianjin 300072, People's Republic of China
E-mail: richardming@tju.edu.cn

Abstract: Walker is a widely used mobility aid to improve users' stability and ambulatory ability. Its dynamometer instrumentation is necessary for quantitative study of basic biomechanics and functional requirements for effective use. How to extract the kinetic demands exactly and without any disturbance to normal gait remains a bottleneck for walker dynamometer design. Based on the force measurement of handle reaction vectors (HRVs) applied to the walker, this study developed a novel strain gauge-based wireless walker dynamometer system integrated with a static calibration algorithm based on ant colony system (ACS). Compared with the traditional measurement of HRV, the proposed method enhances security and flexibility of walker use by using one wireless data transmission system connecting 12 strain-gauge bridges mounted on the walker frame with the computer. To improve high-dimensional calibration performance, an ACS algorithm was employed to optimise the sensitivity weight matrix during calibration. To evaluate force measurement reliability, system performance with ACS algorithm was testified and its mean non-linearity, mean crosstalk and maximal force measurement accuracy error were found to be 6.88, 6.10 and 7.46%, respectively, which were much better than those of traditional linear calibration methods. This implemented walker dynamometer system may prove to be a reliable tool for measurement of hand loads and description of kinetic analysis of basic walker-assisted gait.

1 Introduction

Voluntary mobility is an essential and important demand in activities of daily life for the paraplegic [1] and the elderly [2]. Furthermore, the level of mobility is a good indicator of health status [3]. As a mobility aid tool, the walker provides external mechanical support and reduces weight bearing on lower limbs. Second only to the cane, it is used more often than any other mobility aid [4]. The walker is most helpful for patients with an unstable gait, whose muscles are weak or who require a reduction in the load on weight-bearing structures. In the analysis of basic walker-assisted gait, handle reaction vector (HRV) is very important to document the onset of tremor associated with fatigue, quantify patient stability and identify risk periods within the gait cycle [5]. The potential clinical benefit of HRV measurement is to provide some criteria for evaluation and classification of walking efficiency with walker usage [6].

In several research projects, walkers have been instrumented to quantitate some force components produced by HRV through strain gauges placed on a standard walker frame during the assisted gait cycle. The group of Deathe, Pardo and Winter-measured adult walker reaction forces using strain gauges mounted on the legs of a standard walker [7]. A similar instrumentation method was employed by Fast *et al.* [8] to record forces transmitted through the walker's frame in axial, frontal and sagittal orientations. Force measurements from the walker's handles were designed by Alwan *et al.* [9] to passively assess basic walker-assisted gait characteristics. However, few researchers have focused on exploring the instrumentation method to directly investigate the forces of HRV. A strain gauge-based walker instrumentation system was developed for six degree-of-freedom measurement of resultant HRVs for characterisation of upper extremity loading demands [5]. This system designed with an instrumented handle surface, was so uncomfortable for the users involved that their normal gaits might be influenced or even distorted. Quantification of HRVs could not be made exactly with this system and, therefore full kinetic analysis of walker-assisted walking was not reliable.

This paper developed a wireless dynamometer system with static calibration based on an ant algorithm [ant colony system (ACS)], which provides indirect bilateral measurement of HRV applied by the hands to a walker frame. The specific objective of our study was to design a reliable HRV measurement system to characterise walker-assisted gait kinetics as normal walker use. It is hoped that our design may beneficially influence effective walker use and gait retraining strategies.

2 Methods

2.1 Walker dynamometer

As shown in Fig. 1, the forces applied by the upper body of the user to the walker were defined as HRV. Actually, the

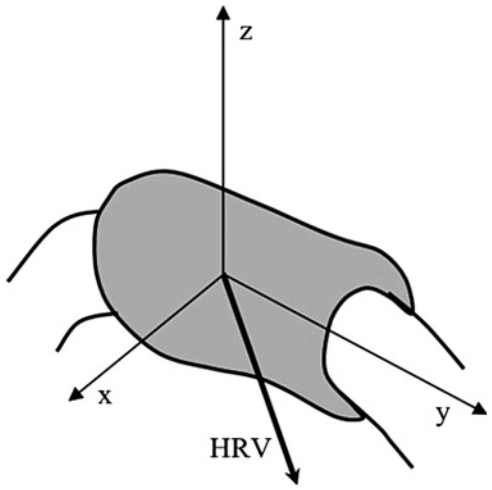

Fig. 1 *Illustration of HRV*

three components of HRV determined the need for additional balance, propulsion and support, respectively, during walker-assisted walking. These handle reaction forces were believed to vary with relevant walking efficiency levels. By gauging resistive strains on walker frame, distortion of walker frame could be quantitatively and efficiently measured.

Twelve strain-gauge bridges, C1–C12, were attached to the walker frame (Fig. 2). FLA-2 series, 350 Ω strain gauges (Tokyo Sokki Kenkyujo Co., Ltd., JP) were employed to be the sensors of this walker. Wheatstone full bridge was used with bending pattern for measurement of bending moments. All strain gauges were oriented such that the bending moments applied on the units could be sensed for analysis. An epoxy-type bonding agent was favoured over cyanoacrylate for long-term stability. The positions of these strain-gauge bridges were determined according to bending moment distributions on walker frame, which were calculated by the finite element analysis method.

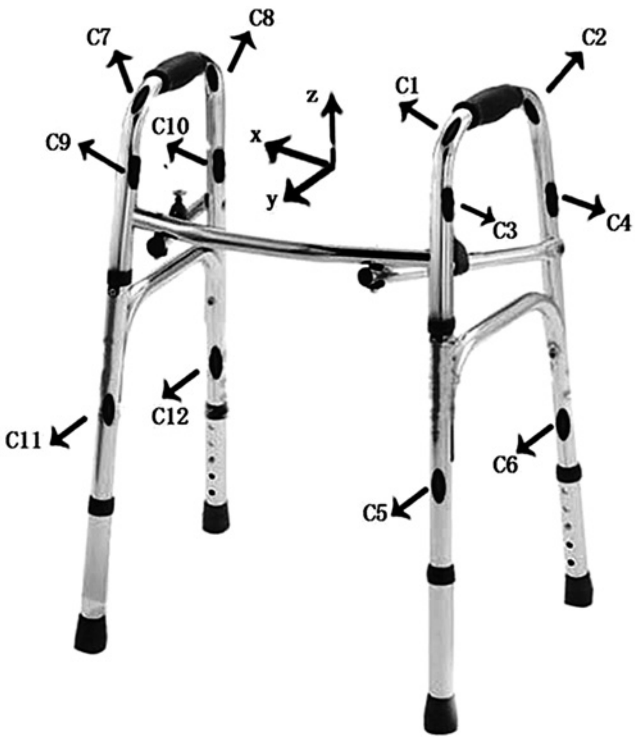

Fig. 2 *Walker instrumentation with 12 strain-gauge bridges*

2.2 Wireless transceiver design

The wireless data transmission system consisted of two parts: sending part and receiving part. The sending part included a CRM2400 module, an ATmega16 Micro Controller Unit (MCU, Atmel Corporation, USA) and batteries. As the core chip of CRM2400, nRF2401 (as shown in Fig. 3) was a single-chip radio transceiver for the 2.4–2.5 GHz industrial, scientific and medical (ISM) band. The sensing data produced by the strain-gauge bridges was amplified and converted into digital signals using 10-bit analogue-to-digital converter, and then input to the ATmega16 MCU. Next, these sensing data were sent out via the CRM2400 module and the receiving part received the data with another CRM2400 module and transmitted them to the PC via a serial port of RS232 for analysing and calculating HRV [10].

2.3 Experimental design

The walker dynamometer system was statically calibrated applying known axial loads, or known forces in another word, unilaterally. Standardised weights were repeatedly hung from cables tied to the middle section of walker handle and were supported by a pulley system designed to minimise frictional losses. To ensure reliability of calibration, the strain gauges were energising for 1 min before the experiment to eliminate temperature interference and each loading was repeated three times. The loading ranges were chosen to reflect the magnitudes of similar forces reported in the literature [11, 12], which were 20 kg along the x-/y-axis and 80 kg along the z-axis, respectively. Therefore when calibrating along x- and y-axis directions, a vertical weight of up to 20 kg was kept on each handle so that frame stability was maintained during calibration.

2.4 Calibration methods

2.4.1 Traditional linear fitting: Linear calibration of walker dynamometer system was available based on the hypothesis that there was a strictly linear relationship between HRV and the outputs of strain-gauge bridges. This meant that gauge sensitivity was determined by linearising the output voltages with respect to the known applied loads. System behaviour was characterised by using the equation

$$\boldsymbol{V} = \boldsymbol{C}\boldsymbol{F} \tag{1}$$

where $\boldsymbol{V}$ was a column vector representing output voltages from strain-gauge bridges and $\boldsymbol{F}$ was a column vector representing applied loads. Sensitivity weight matrix $\boldsymbol{C}$ related applied loads to measured outputs. The sensitivity weight matrix was also written as follows

$$\boldsymbol{C} = \left[\boldsymbol{V}_{\rm lx}/\boldsymbol{F}_{\rm lx}, \boldsymbol{V}_{\rm ly}/\boldsymbol{F}_{\rm ly}, \boldsymbol{V}_{\rm lz}/\boldsymbol{F}_{\rm lz}, \boldsymbol{V}_{\rm rx}/\boldsymbol{F}_{\rm rx}, \boldsymbol{V}_{\rm ry}/\boldsymbol{F}_{\rm ry}, \boldsymbol{V}_{\rm rz}/\boldsymbol{F}_{\rm rz}\right] \tag{2}$$

where $\boldsymbol{V}_{\rm lx}/\boldsymbol{F}_{\rm lx}$, $\boldsymbol{V}_{\rm ly}/\boldsymbol{F}_{\rm ly}$ and $\boldsymbol{V}_{\rm lz}/\boldsymbol{F}_{\rm lz}$ were sensitivity column vectors at x-, y- and z-directions of left HRV, respectively, and so were $\boldsymbol{V}_{\rm rx}/\boldsymbol{F}_{\rm rx}$, $\boldsymbol{V}_{\rm ry}/\boldsymbol{F}_{\rm ry}$ and $\boldsymbol{V}_{\rm rz}/\boldsymbol{F}_{\rm rz}$ of right HRV.

As shown in Fig. 4 for traditional linear fitting method, x-coordinate represented the value of the force exerted on

doi: 10.1049/iet-wss.2012.0136

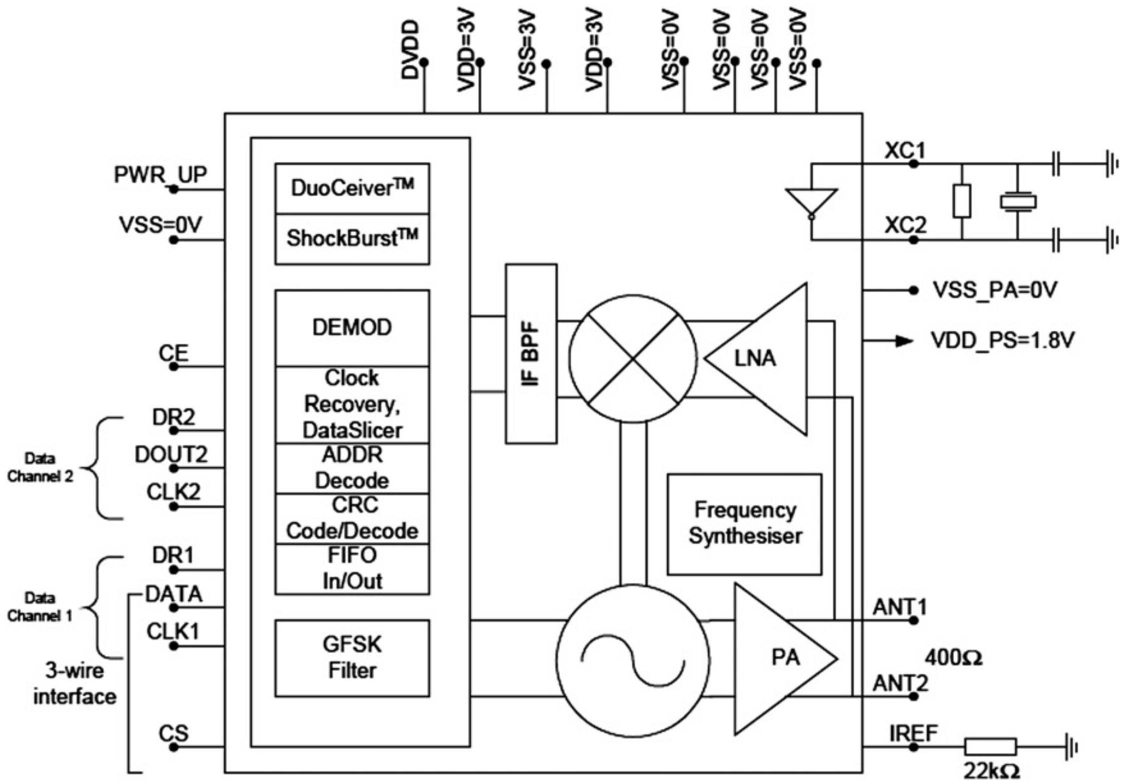

Fig. 3 *nRF2401 with external components*

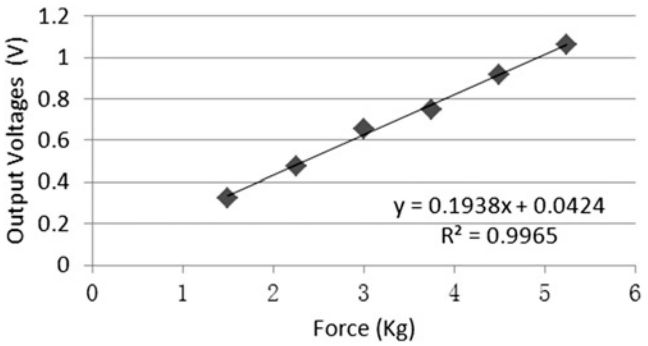

Fig. 4 *Sensitivity weight V_1/F_{lx} calculation*

the walker handle in $\boldsymbol{F}_{lx}$ direction of HRV, and y-coordinate represented the output V_1 of strain-gauge bridge $C1$ of the dynamometer system. Slope coefficient $V_1/\boldsymbol{F}_{lx}$ of trend line was 0.1938. The slope coefficients of $V_2/\boldsymbol{F}_{lx}$, $V_3/\boldsymbol{F}_{lx}$ to $V_{12}/\boldsymbol{F}_{lx}$ were computed the same way as $V_1/\boldsymbol{F}_{lx}$. Then, sensitivity weight matrix $\boldsymbol{C}$ could be determined by (2). Therefore HRV could be solved from the following formula

$$\boldsymbol{F} = \boldsymbol{C}^{-1}\boldsymbol{V} \tag{3}$$

where calculation of $\boldsymbol{C}^{-1}$ was based on (Moore–Penrose) pseudoinverse of $\boldsymbol{C}$.

This method was reliable under the hypotheses that the dynamometer system was linear. Owing to the complicated principle of non-linear strain gauges, this method had some limitations on calibration accuracy. To eliminate these limitations, ACS was used in this calibration.

2.4.2 Ant colony system: To improve the calibration performance of the walker dynamometer, an algorithm of ACS was developed and tested to determine the sensitivity weight matrix as defined $\boldsymbol{C}^{-1}$ in (3). ACS was developed on the basis of the ant algorithm as a promising multi-agent approach to difficult combinatorial optimisation problems such as the travelling salesman problem [13] and the quadratic assignment problem [14].

In this study, we concentrated on binary ACS because binary representation was the most efficient and economical data representation, and two-value logic was the easiest way to simulate and implement in nature [15]. Every element of $\boldsymbol{C}^{-1}$ was transformed into nine binary digits, and the first digit represented the sign of the element. Totally, 118 binary digits could express one row of $\boldsymbol{C}^{-1}$ which was related to one component of HRV independently.

When ACS produced $\boldsymbol{C}_i^{-1}$ (the ith row of $\boldsymbol{C}^{-1}$), F_i (the ith element of $\boldsymbol{F}$) was obtained by $\boldsymbol{C}_i^{-1} \cdot \boldsymbol{V}$. Supposing F_i was the calculated result and F_i' was the actual force exerted on the handle. In the algorithm used here, $|F_i - F_i'|$ was the objective function. As the algorithm looped, the value of $|F_i - F_i'|$ decreased. The goal was to make $|F_i - F_i'|$ as small as possible, that is to say, an appropriate $\boldsymbol{C}_i^{-1}$ needed to be found to make F_i close to F_i'. $E_{\min}$, which was properly small, was set to limit $|F_i - F_i'|$. When $|F_i - F_i'| < E_{\min}$, it broke the loop, and final $\boldsymbol{C}^{-1}$ was determined through the cycle.

To describe the calibration process of ACS, details of how the sensitivity weight matrix was determined by the binary ACS were shown in Fig. 5. During the process of ACS calibration, the ant chose the route according to the remaining pheromone, which was updated by some principles discussed as below.

ACS employed a local pheromone update, in addition to the pheromone update at the end of each epoch. Each ant

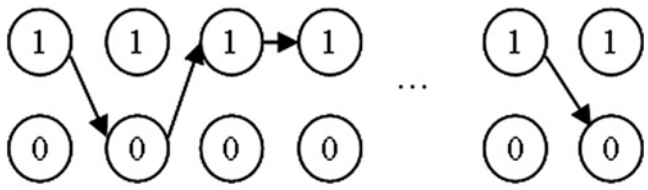

Fig. 5 *Searching route of ACS for* $\boldsymbol{C}^{-1}$

performed the pheromone update after each construction step, applying pheromone to the last path traversed according to the local pheromone update function [16]

$$\tau_{ij} = (1-\xi)\tau_{ij} + \xi\tau_0 \tag{4}$$

where τ_{ij} was the quantity of the pheromone laid on path (i, j), τ_0 was the initial value of the pheromone and $\xi \in (0, 1]$ was pheromone decay coefficient. In our research, i and j were neighbouring digits in one row of $\boldsymbol{C}^{-1}$ with a value of 0 or 1.

The global update was applied at the end of each epoch by the iteration-best or the best-so-far ant only. The update function for global pheromone update was as follows [16]

$$\tau_{ij} = \begin{cases} (1-\rho)\tau_{ij} + \rho\Delta\tau_{ij}, & \text{if ant } (i, j) \text{ belongs to best route} \\ 0, & \text{otherwise} \end{cases} \tag{5}$$

$\Delta\tau_{ij} = (1/L_{\text{best}})$, where L_{best} was the length of the best route, and $\rho \in (0, 1]$. The complete epoch meant determination of one row (118 digits) by this method. The length of the best route referred to the minimum value of objective function, hence searching for the best route meant looking for appropriate $\boldsymbol{C}_i^{-1}$ which led to the most approaching calculated force comparing the real one.

The ant chose paths according to the pseudorandom proportional rule. If we let k be an ant located at state i, probability of the ant k making the transition from state i to state j was given by (6).

$$j = \begin{cases} \arg\max \tau_{ij}(t)\left[\eta_{ij}(t)\right]^{\beta}, & \text{if} \quad q \le q_0 \\ S, & \text{else} \end{cases} \tag{6}$$

where $q \in [0, 1]$ was a random value, and $q_0 \in [0, 1]$ was a constant. η_{ij}, the visibility of state j from state i, was defined as

$$\eta_{ij} = \frac{1}{\text{distance}(i, j)} \tag{7}$$

This parameter η_{ij} was utilised to prevent local convergence, which helped in approaching the optimal solution of the problem. j was more likely to be chosen as the next state when the parameters τ_{ij} and η_{ij} were increasing. Visibility was weighted by parameter β and the following formula (where $p_{ij}^k(t)$ was the probability of choosing state j from state i at time t and allowed$_k$was the set of states that were still allowed for ant k) was arrived [17]

$$p_{ij}^k(t) = \begin{cases} \dfrac{\tau_{ij}(t)\cdot\left[\eta_{ij}(t)\right]^{\beta}}{\sum \tau_{ij}(t)\cdot\left[\eta_{ij}(t)\right]^{\beta}}, & \text{if} \quad j \in \text{allowed}_k \\ 0, & \text{else} \end{cases} \tag{8}$$

3 System reliability test results

To evaluate HRV measurement reliability, system performance was verified in this paper via non-linearity validation, crosstalk test and force measurement error check. All these tests were based on the hypothesis that the walk frame was rigid.

3.1 *Non-linear error*

Non-linear error was defined as (9)

$$E_i = \left|\frac{D_{\max}}{F_{\text{full}}}\right| \times 100\% \tag{9}$$

where i was the index of the direction, $D_{\max}$ was max difference value (D-value) between measurement results and real values in this direction and F_{full} was full-range load in the same direction [18]. Totally six non-linear errors, namely $i = 1$–6, were measured in the left and right x-, y- and z-directions. Non-linear errors with linear and ACS calibration methods along all directions were tabulated in Table 1. It could be seen that non-linear errors with linear and ACS calibration methods were <20.75 and 9.16%, respectively, and the mean of the non-linear errors in six directions of ACS was 6.88%, less than that of linear fitting (8.99%).

3.2 *Crosstalk*

When a force was exerted along one direction of the walker frame, for example, left X, at the walker handle, there were fake force outputs in the other five directions except for left X direction. This phenomenon was called crosstalk, which was determined as

$$\text{CT}_{i-j} = \left|\frac{F_i}{F_j}\right| \times 100\% \tag{10}$$

where i was the measured fake force direction, j was the force exerting direction, F_i was the fake force output along i-direction, F_j was exerting force along j-direction and CT_{i-j} was the crosstalk between i and j directions. Five crosstalks were calculated when exerting a force in one direction. The maximum one was defined as crosstalk in the force exerting direction. Crosstalks with linear and ACS calibration methods along all directions were tabulated in

Table 1 Non-linear errors with linear fitting and ACS calibration (%)

Calibration method	F_{lx}	F_{ly}	F_{lz}	F_{rx}	F_{ry}	F_{rz}	Mean
linear fitting	3.76	6.30	11.55	**20.75**	5.01	6.59	8.99
ACS	**9.16**	7.13	5.22	8.26	3.56	7.92	6.88

IET Wirel. Sens. Syst., 2013, Vol. 3, Iss. 3, pp. 233–238
doi: 10.1049/iet-wss.2012.0136

Table 2 Crosstalks with ACS (and linear fitting) calibration (%)

Force direction		Fake forces						Crosstalk	Mean crosstalk
		Left HRV			Right HRV				
		F_x	F_y	F_z	F_x	F_y	F_z		
Left HRV	F_x	/	0.88 (1.04)	0.03 (2.13)	2.74 (4.45)	0.97 (2.84)	0.92 (0.88)	2.74 (4.45)	6.10 (15.85)
	F_y	2.41 (4.14)	/	1.14 (0.96)	0.78 (5.22)	2.52 (1.66)	0.34 (0.16)	2.52 (5.22)	
	F_z	4.15 (0.92)	9.16 (9.22)	/	11.97 (32.66)	1.23 (1.11)	0.16 (3.33)	**11.97 (32.66)**	
Right HRV	F_x	0.72 (10.90)	4.67 (2.18)	1.68 (2.33)	/	0.46 (1.99)	1.53 (2.92)	4.67 (10.90)	
	F_y	1.49 (2.10)	2.88 (2.10)	1.01 (0.13)	2.81 (9.92)	/	0.33 (0.06)	2.88 (9.92)	
	F_z	6.22 (23.73)	7.23 (25.47)	0.94 (0.59)	4.62 (31.96)	11.80 (15.67)	/	11.80 (31.96)	

Table 2. It could be seen that mean crosstalks with linear and ACS calibration methods were 15.85 and 6.10%, respectively.

3.3 Accuracy

To verify the accuracy of this system, a reference force F_c was exerted at the handle of the walker frame in arbitrary direction. HRV forces were calculated from the outputs of strain-gauge bridges. Thus, the resultant force measured by the walker system was calculated by

$$F_r = \sqrt{F_x^2 + F_y^2 + F_z^2} \tag{11}$$

where $F_x = F_{lx} + F_{rx}$, $F_y = F_{ly} + F_{ry}$, $F_z = F_{lz} + F_{rz}$. The force accuracy error was calculated by

$$E_r = \left| \frac{F_r - F_c}{F_c} \right| \times 100\% \tag{12}$$

where F_c was a real force which was exerted in a random direction, F_r was the measurement force calculated from the

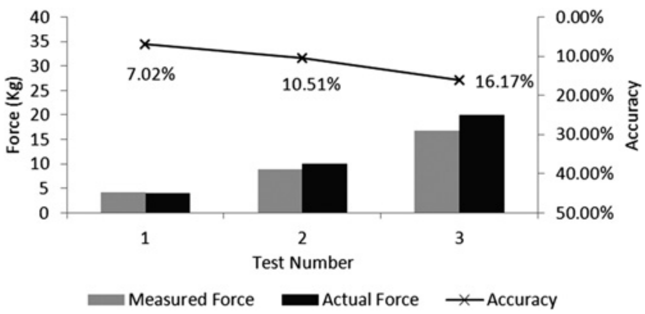

Fig. 6 *Force accuracy errors of linear fitting calibration*

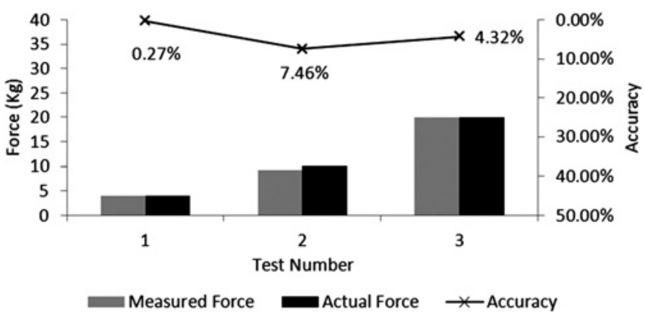

Fig. 7 *Force accuracy errors of ACS calibration*

outputs of strain-gauge bridges. Force accuracy errors with linear and ACS calibration methods were shown in Figs. 6 and 7. It could be seen that force accuracy errors with linear and ACS calibration methods were <16.17 and 7.46%, respectively.

4 Discussion

Currently, all dynamometer systems designed for walker-assisted walking employ the direct force measurement method, meaning that the loads were sensed on the walker handles and transmitted to the computer through wires. However, in view of the effective usage of the walker, the wireless pattern should be favoured in walker dynamometer system because of the following advantages: (i) no wires meant less possibility for user to stumble and lower risk of falling down; (ii) users could walk free and reach larger scale without the wires' limit. Therefore the wireless system proposed in this study enhances security and flexibility of walker use, which are the basic requirements of rehabilitation aids.

Critical calibration is essential for walker instrumentation to get better and more reliable force measurement results. Since sensitivity weight matrix of the force sensing elements was only determined by simple linear fitting on the basis of a large group of experimental data, the traditional linear fitting method could not guarantee robust and complex-optimised results during high-dimensional matrix. To address these problems, an ACS-based swarm intelligence strategy was introduced to optimise sensitivity weight matrix of walker dynamometer calibration.

Considering the test results of the above method, system non-linearity, crosstalk and accuracy with ACS calibration were all much better than those with linear fitting calibration, which verified the advantages of ACS in optimising information fusion progress for multi-sensors in walker dynameters system. Similar to the traditional linear fitting calibration, ACS calibration was also fit for a real-time system simply by producing a sensitivity weight matrix. The adjustable parameters were set by ant rules and calibration experiments. Once the sensitivity weight matrix and the accuracy of every element were determined, the number of states was fixed (assuming that it was N). As addressed in [19], the number of ants m was 1.5 times of N. In addition, the parameters ρ_0, τ_0 and ξ were determined by grid method where the interval between each value was 0.2. In future work, these three parameters could be optimised with more calculations to achieve smaller errors, or an optimisation algorithm could be applied to adjust the three parameters, for example, genetic algorithm (GA). The GA method may be used to find proper parameters of ACS, which is known as fusion of the GA and ant algorithm.

5 Conclusions

In this paper, a new dynamometer system was investigated to measure HRV accurately and wirelessly during walker-assisted walking, which made it possible to analyse the biomechanics and monitor walking efficiency of walker users. The focus of this paper is on description and experimental testing of this system.

Indirect measurement based on 12 strain-gauge bridges relieved walker users' sufferings from uncomfortable instrumented handles and eliminated the influence of hands on strain gauges. By using the CRM2400 wireless module, the transceiver transmitted the data from the sensor network of strain-gauge bridges mounted on the walker frame to the computer. Then, HRV information was extracted from these data by a novel calibration algorithm of ACS. The testing results show that significant improvements were achieved by the proposed calibration based on ACS. Compared with the traditional linear fitting method, the proposed calibration method with ACS showed smaller non-linear error (6.88 against 8.99%), lower crosstalk (6.10 against 15.85%) and smaller force accuracy error (7.46 against 16.17%) in this study.

With further clinical applications, the proposed system could be employed as (i) evaluation of walker-assisted walking performance, (ii) assessment of muscle characteristics and (iii) supply of a feedback signal to choose an efficient walking pattern for other rehabilitation techniques, for example, functional electrical stimulation.

6 Acknowledgment

The authors would like to acknowledge Gait-lab of Duchess of Kent Children's Hospital (Hong Kong SAR, China) and Prof. Hu Y, Prof. Leong JCY, Prof. Luk KDK, Dr. Wong YW and Dr. Lu WWJ for their valuable contributions to this research. This research was partially supported by the National Natural Science Foundation of China (No. 81222021, 30970875, 90920015, 61172008 and 81171423), National Key Technology R&D Programme of the Ministry of Science and Technology of China (No. 2012BAI34B02) and Programme for New Century Excellent Talents in University of the Ministry of Education of China (No. NCET-10-0618).

7 References

1 Ming, D., Bai, Y.R., Liu, X.Y., *et al.*: 'A gait stability investigation into FES-assisted paraplegic walking based on the walker tipping index', *J. Neural Eng.*, 2009, **6**, (6), pp. 066007

2 Alwan, M., Jude Rajendran, P., Ledoux, A., Huang, C., Wasson, G., Sheth, P.: 'Stability margin monitoring in steering-controlled intelligent walkers for the elderly'. AAAI Fall Symp., 2005

3 Scanaill, C.N., Carew, S., Barralon, P., Noury, N., Lyons, D., Lyons, G.M.: 'A review of approaches to mobility telemonitoring of the elderly in their living environment', *Ann. Biomed. Eng.*, 2006, **34**, (4), pp. 547–563

4 Stallard, J.: 'Walking for the severely disabled', *J. Bone Joint Surg.*, 2005, **87-B**, (5), pp. 604–607

5 Bachschmidt, R.A., Harris, G.F., Simoneau, G.G.: 'Walker-assisted gait in rehabilitation: a study of biomechanics and instrumentation', *IEEE Trans. Neural Syst. Rehabil. Eng.*, 2001, **9**, (1), pp. 96–105

6 Cole, L., Powell, R., Danial, D.: 'The effects of upper body weight support upon cardiovascular, metabolic and electromyographic variables during assisted walking', *Int. J. Rehabil. Res.*, 2000, **23**, (11), pp. 129–134

7 Deathe, A.B., Pardo, R.D., Winter, D.A.: 'Stability of walking frames', *J. Rehabil. Res. Dev.*, 1996, **33**, (1), pp. 30–35

8 Fast, A., Wang, F.S., Adrezin, R.S., Cordaro, M.A., Ramis, J., Sosner, J.: 'The instrumented walker: usage patterns and forces', *Arch. Phys. Med. Rehabil.*, 1995, **76**, (5), pp. 484–494

9 Alwan, M., Ledoux, A., Wasson, G., Sheth, P., Huang, C.: 'Basic walker-assisted gait characteristics derived from forces and moments exerted on the walker's handles: results on normal subjects', *Med. Eng. Phys.*, 2007, **29**, pp. 380–389

10 Wang, Y., Zhang, R., Li, D., Hu, Y., Ming, D., Wan, B.: 'Study on wireless data transmission for dynamometer walker system'. VECIMS 2009 – Int. Conf. on Virtual Environments, Human-Computer Interface and Measurements Systems, Hong Kong, China, May 2009, pp. 232–235

11 Pardo, R.D., Winter, D.A., Deathe, A.B.: 'System for routine assessment of walker-assisted gait', *Clin. Biomech.*, 1993, **8**, (2), pp. 73–80

12 Fast, A., Wang, F.S., Adrezin, R.S., Cordaro, M.A., Ramis, J., Sosner, J.: 'The instrumented walker: usage patterns and forces', *Arch. Phys. Med. Rehabil.*, 1995, **76**, (5), pp. 484–491

13 Dorigo, M., Gambardella, L.M.: 'Ant colony system: a cooperative learning approach to the travelling salesman problem', *IEEE Trans. Evol. Comput.*, 1997, **1**, (1), pp. 53–66

14 Maniezzo, V., Colorni, A.: 'The ant system applied to the quadratic assignment problem', *IEEE Trans. Knowl. Data Eng.*, 1999, **11**, (5), pp. 769–778

15 Xiong, W.Q., Wang, L.Y.: 'Binary ant colony algorithm with transferring the signal'. Fifth Int. Conf. on Machine Learning and Cybernetic, Dalian, China, August 2006, pp. 2148–2153

16 Mullen, R.J., Monekosso, D., Barman, S., Remagnino, P.: 'A review of ant algorithms', *Expert Syst. Appl.*, 2009, **36**, (6), pp. 9608–9617

17 Gaertner, D., Clark, K.: 'On optimal parameters for ant colony optimization algorithms'. Int. Conf. on Artificial Intelligence, Las Vegas, Nevada, USA, June 2005, pp. 83–89

18 Ming, D., Liu, X.Y., Bai, Y.R., *et al.*: 'Measurement of upper extremity joint moments in walker-assisted gait', *IET Sci. Meas. Technol.*, 2009, **3**, (5), pp. 343–353

19 Duan, H.: '*Ant colony algorithms theory and applications*' (Science Press, 2005, 1st edn.)

doi: 10.1049/iet-wss.2012.0136